Heliyon 10 (2024) e24235

Contents lists available at ScienceDirect

Heliyon

journal homepage: www.cell.com/heliyon

Research article

Modification patterns and metabolic characteristics of m^{6}A regulators in digestive tract tumors

Bing He [1], Yiyang Hu [1], Hui Chen, Xia Xie, Chunli Gong, Zhibin Li, Yang Chen, Yufeng Xiao [**], Shiming Yang [*]

Department of Gastroenterology, Xinqiao Hospital, Army Military Medical University, Chongqing, 400037, China

ARTICLE INFO

Keywords:
m6A
Epigenetics
Digestive
Tumor
Metabolism

ABSTRACT

M6A is essential for tumor occurrence and progression. The expression patterns of m6A regulators differ in various kinds of tumors. Transcriptomic expression statistics together with clinical data from a database were analyzed to distinguish patients with digestive tract tumors. Based on the expression patterns of diverse m6A regulators, patients were divided into several clusters. Survival analysis suggested significant differences in patient prognosis among the m6A clusters. The results showed overlapping of m6A expression patterns with energy metabolism and nucleotide metabolism. Functional analyses imply that m6A modifications in tumor cells probably drive metabolic reprogramming to sustain rapid proliferation of cancer cells. Our analysis highlights the m6A risk characterizes various kinds of metabolic features and predicts chemotherapy sensitivity in digestive tract tumors, providing evidence for m6A regulators as markers to predict patient outcomes.

1. Introduction

Originating from the endoderm, digestive tract tumors are common types of malignant tumors and are a leading cause of cancer deaths worldwide [1]. Esophageal adenocarcinoma (ESCA), stomach adenocarcinoma (STAD), colon adenocarcinoma (COAD) and rectal adenocarcinoma (READ) are the main types of digestive tract tumors. Early symptoms of digestive tract tumors are not noticeable until they enter advanced and malignant stages, making them difficult to diagnose early [2,3]. However, with the advances in technology, regular medical checkups and screening of patients, the early diagnosis rate of tumors is increasing year by year. The survival rates of these patients have also improved in recent years, but the prognosis of patients remains unsatisfactory [4,5].

M6A modification is the most prevalent posttranscriptional modification in mRNA of eukaryotic organisms, and the biological regulation of this modification is now widely understood and well-studied [6–8]. M6A modification is regulated dynamically by "writers", "erasers" and "readers". M6A modification has multiple regulatory effects on various cellular biological behaviors [9,10]. The mechanisms associated with m6A in digestive tract tumors have been widely reported. HNRNPA2B1 enhances the expression of

* Corresponding authors. Department of Gastroenterology, Xinqiao Hospital, Army Military Medical University, No.183, Xinqiao Main ST, Shapingba District, 12 Chongqing 400037, China.

** Corresponding authors. Department of Gastroenterology, Xinqiao Hospital, Army Military Medical University, No.183, Xinqiao Main ST, Shapingba District, 12 Chongqing 400037, China.

E-mail addresses: xiaoyufeng@tmmu.edu.cn (Y. Xiao), yangshiming@tmmu.edu.cn (S. Yang).

[1] Bing He and Yiyang Hu contributed equally to this work.

https://doi.org/10.1016/j.heliyon.2024.e24235
Received 14 November 2023; Received in revised form 29 November 2023; Accepted 4 January 2024
Available online 14 January 2024

ACLY and ACC1 to promote ESCA progression [11]. METTL14 inhibits the growth and metastasis of STAD by regulating m6A modification of PTEN mRNA [12]. Cell cycle and angiogenesis are modulated by IGF2BP3 in COAD [10]. In READ, METTL14 was identified as a favorable prognostic biomarker [13]. Different m6A regulators are expressed at different levels in different tumors and perform various functions. It is urgent to reprofile patients to more profoundly understand the role of m6A in digestive tract tumors.

Metabolic reprogramming is a hallmark of cancer, and metabolic therapy is an extremely promising target to prevent tumor development. However, heterogeneous metabolism exists across tumor types and different evolutionary stages [14,15]. Metabolic heterogeneity hinders the effects of metabolism-targeting drugs [16]. M6A modification enable tumor cells to acquire specific metabolic phenotypes [17,18]. M6A regulators may therefore represent targets for metabolic assessment and tumor treatment.

In this paper, we collected RNA expression profile from database and clustered digestive tract tumors by their m6A expression patterns. The clinical features of individual tumors were evaluated among the different clusters. The results revealed that the survival of patients differed significantly among clusters. Functional analysis even suggested metabolism enrichment in some clusters, suggesting the significance of m6A risk and metabolism risk for guiding the clinical treatment of patients and providing a marker to predict patient outcomes.

2. Methods

2.1. Dataset source and preprocessing

Gene expression data and genetic information together with clinical features were obtained from The Cancer Genome Atlas (TCGA) database using the R package TCGAbiolinks. We also selected expression profiles from the Gene-Expression Omnibus (GEO) dataset to validate relevant results. Patients without survival information were excluded from further evaluation. We converted FPKM values in the data to transcripts per kilobase million (TPM) values using the "ComBat" algorithm of the sva package to correct for the bulk effect of non-biotech bias. We collected a total of 25 m6A regulate genes. 9 writers including (METTL3, METTL14, METTL16, RBM15, RBM15B, WTAP, KIAA1429, CBLL1, ZC3H13). 14 readers including (YTHDC1-2, YTHDF1-3, IGF2BP1-3, HNRNPA2B1, HNRNPC, RBMX, FMR, LRPPRC, ELAVL1) and 2 erasers (ALKBH5, FTO).

2.2. Interaction between m6A regulators

Univariate cox regression analysis was used to evaluate the prognostic status of 25 regulators on four kinds of tumors. Those selected with $p < 0.05$ were considered to be associated with survival. The prognostic network was constructed based on the hazard ratio (HR) values of these regulators.

2.3. Consensus unsupervised clustering analysis for m6A regulators

The R package "ConsensusClusterPlus" was adopted to divide patients into several groups according to the expression pattern of 25 m6A regulators [19]. The cumulative distribution function (CDF) was changed under variation of k value. Judgment of propriate k value was made based on the increasing area under the CDF curve.

2.4. Metabolic signature analysis

Components of the metabolism-associated genes were obtained from a previous report [20]. Gene list was provided in Supplementary Table 1.

2.5. M6A risk scoring system

Principal component analysis (PCA) was performed to visualize the two-dimensional distribution of clusters. Subsequently, the empirical Bayesian approach of the limma R package was applied to distinguish differentially expressed genes (DEGs) among clusters. Then, univariate Cox regression analysis was performed to retain genes with $P < 0.05$ based on the upper differential genes obtained. We then performed PCA to construct m6A-associated gene profiles. M6A risk values were constructed using the formula:

$$\text{m6Ascore} = \sum_{i=1}^{k} (PC1 \times exp_i + PC2 \times exp_i)$$

where exp is the expression of the associated gene obtained by least absolute shrinkage and selection operator (LASSO) regression. TCGA acted as the test cohort, while GEO acted as the validation cohort.

2.6. Prediction of drug sensitivity by m6A score

Drug IC50 was predicted based on GDSC database cell line expression profiles and TCGA gene expression profiles using the R package "oncoPredict" algorithm. The correlation between drug IC50 and the m6A score constructed above was analyzed.

2.7. Statistical analyses

All data processing and statistical analysis were performed using R (3.6.1) and GraphPad Prim 9. Non-parametric Kruskal-Wallis and Wilcoxon rank-sum tests were used to determine the differences of variables in each group. A one-way COX-analysis of m6A regulators and metabolites was used to assess patient prognosis. The correlations were quantified using Pearson correlation coefficients. The timeROC package was used to estimate the specificity and sensitivity of m6Ascore in the test and validation sets. The survival curves were generated using the Kaplan-Meier method and the significance of the differences was determined using a log-rank test. All statistical P-values were bilateral and were considered significant at $P < 0.05$.

3. Results

3.1. Genetic variation and expression of m6A regulators in digestive tract tumors

Twenty-five m6A regulators were identified in digestive tract tumors, including ESCA, STAD, COAD and READ. First, we analyzed the expression of these 25 regulators among the four kinds of tumors (Fig. 1A–D). Surprisingly, all regulators showed significant differences in expression in STAD (Fig. 1B) but fewer differences in expression in READ (Fig. 1D). Among the regulators, most of them had consistently higher expression in tumor samples, such as METTL3, CBLL1, YTHDF1, IGF2BP1, HNRNPA2B1, LRPPRC and ELAVL1

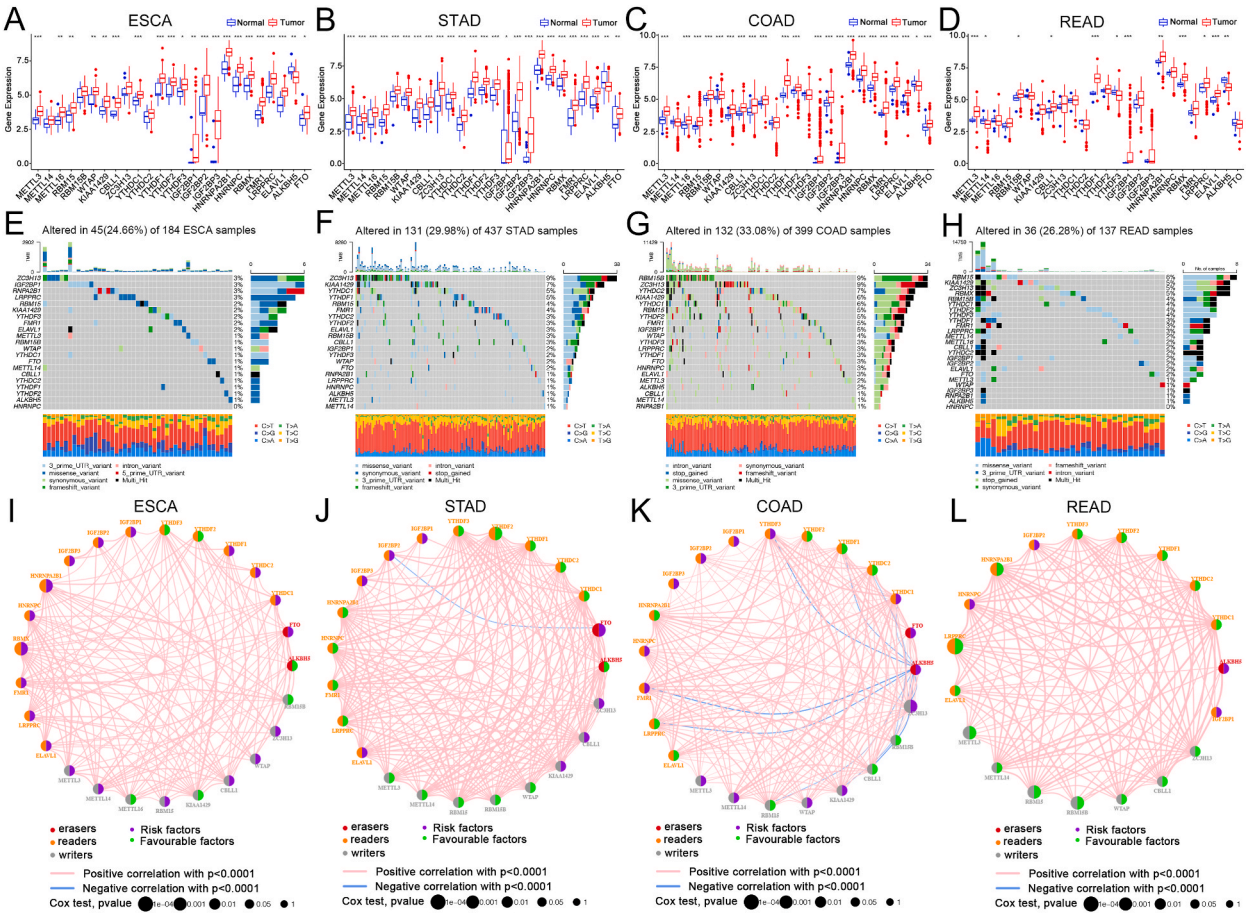

Fig. 1. Landscape of genetic variation and mRNA expression levels of 25 m6A regulators. (A–D) Expression of 25 m6A regulators between normal and tumor tissues in ESCA, STAD, COAD and READ. Tumors are in red; normal is in blue. The upper and lower ends of the box plots represent the interquartile range of values. The lines in the boxes represent medians and the dots indicate outliers. Asterisks represent statistical P values (*$P < 0.05$; **$P < 0.01$; ***$P < 0.001$). (E–H) Mutation frequencies of m6A regulators in ESCA, STAD, COAD and READ. Each column represents an individual patient, the bar above shows the TMB, and the numbers on the right indicate the mutation frequency of each regulator. The right bar shows the proportion of each variant type, and the stacked bars below show the conversion rate in each sample. (I–L) The circle size represents the effect of each regulator on prognosis, and the values calculated by Log-rank test range from $P < 0.0001$, $P < 0.001$, $P < 0.01$, $P < 0.05$, and $P < 1$. The colors in the circles represent the gene type and risk gene type of m6A. The lines connecting the regulators indicate their interactions, and the thickness indicates the strength of the correlation between the regulators. Negative correlations are marked in blue and positive correlations are marked in pink. (For interpretation of the references to color in this figure legend, the reader is referred to the Web version of this article.)

($p < 0.05$). In contrast, ALKBH5 showed significantly higher expression in normal tissues ($p < 0.05$) (Fig. 1A–D). The highly heterogeneous expression profile of m6A regulators suggested that imbalance in m6A regulator expression plays a key function in the development and advancement of digestive tract tumors.

To compare the differences in m6A regulators at the genetic level, the somatic mutations and copy number variation (CNV) results were evaluated (Fig. 1E–H, Fig. S1). The frequencies of the mutations in these four tumors were 24.46 %, 29.98 %, 33.08 % and 26.28 %, respectively. COAD showed the highest variation rate. ZC3H13 exhibited the highest mutation rate in ESCA and STAD and ranked second in COAD and third in READ. KIAA1429, RBM15 and RBM15B were also highly ranked among these tumors. Among the

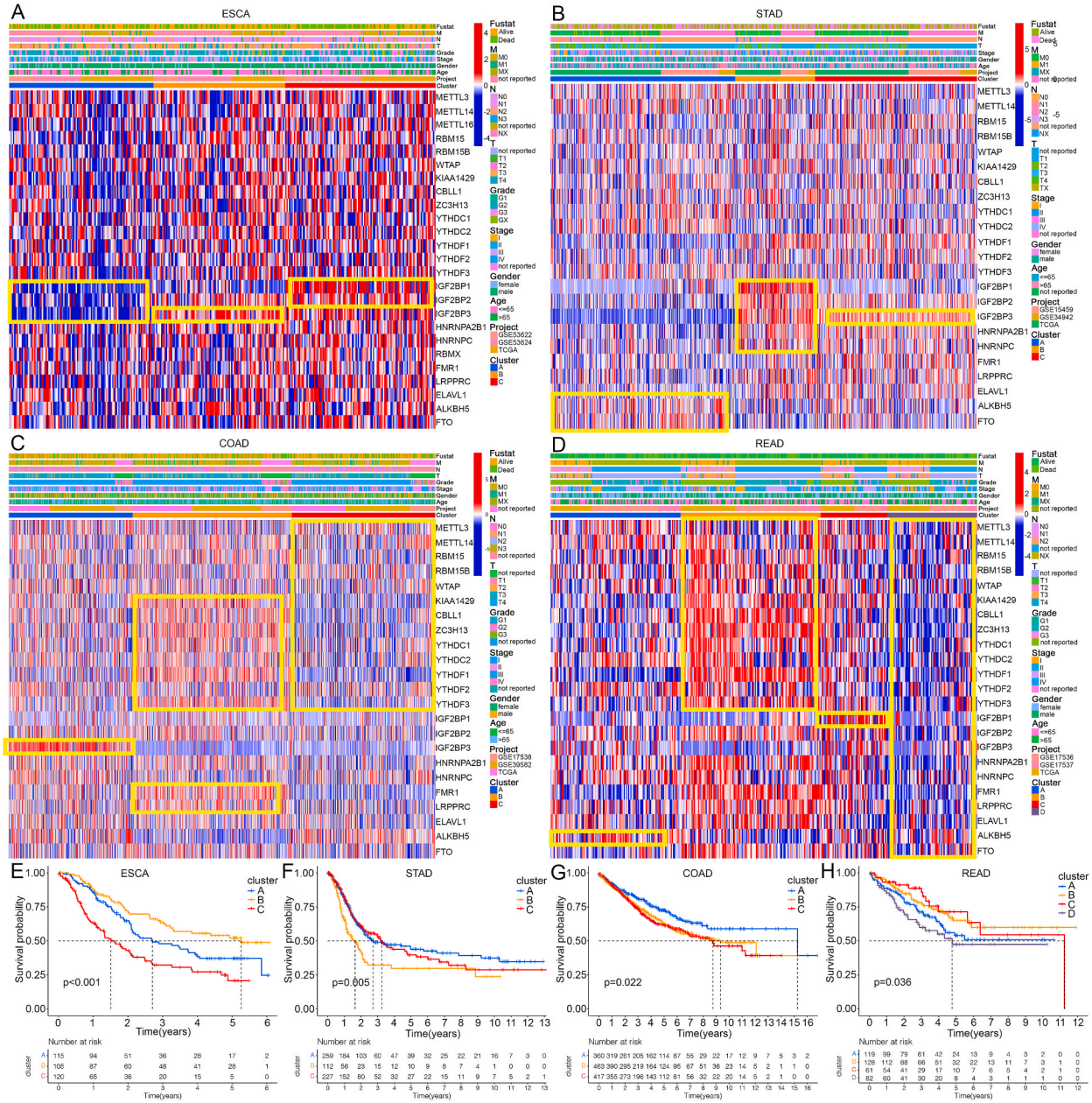

Fig. 2. Consensus cluster of m6A regulators based on their expression pattern. (A–D) Unsupervised clustering of 25 m6A genes in ESCA, STAD, COAD and READ. cluster, survival status, age, gender, stage, grade and other clinical features were shown. Red represents high expression of regulatory factors; blue represents low expression. (E) The survival analysis was performed for the three m6A modification patterns in ESCA. Kaplan-Meier curve with a log-rank p-value<0.001 showed a significant survival difference between the three m6A modification patterns. (F) Kaplan-Meier curve with a log-rank p-value = 0.005 in STAD. (G) Kaplan-Meier curve with a log-rank p-value = 0.022 in COAD. (H) Kaplan-Meier curve with a log-rank p-value = 0.036 in READ. (For interpretation of the references to color in this figure legend, the reader is referred to the Web version of this article.)

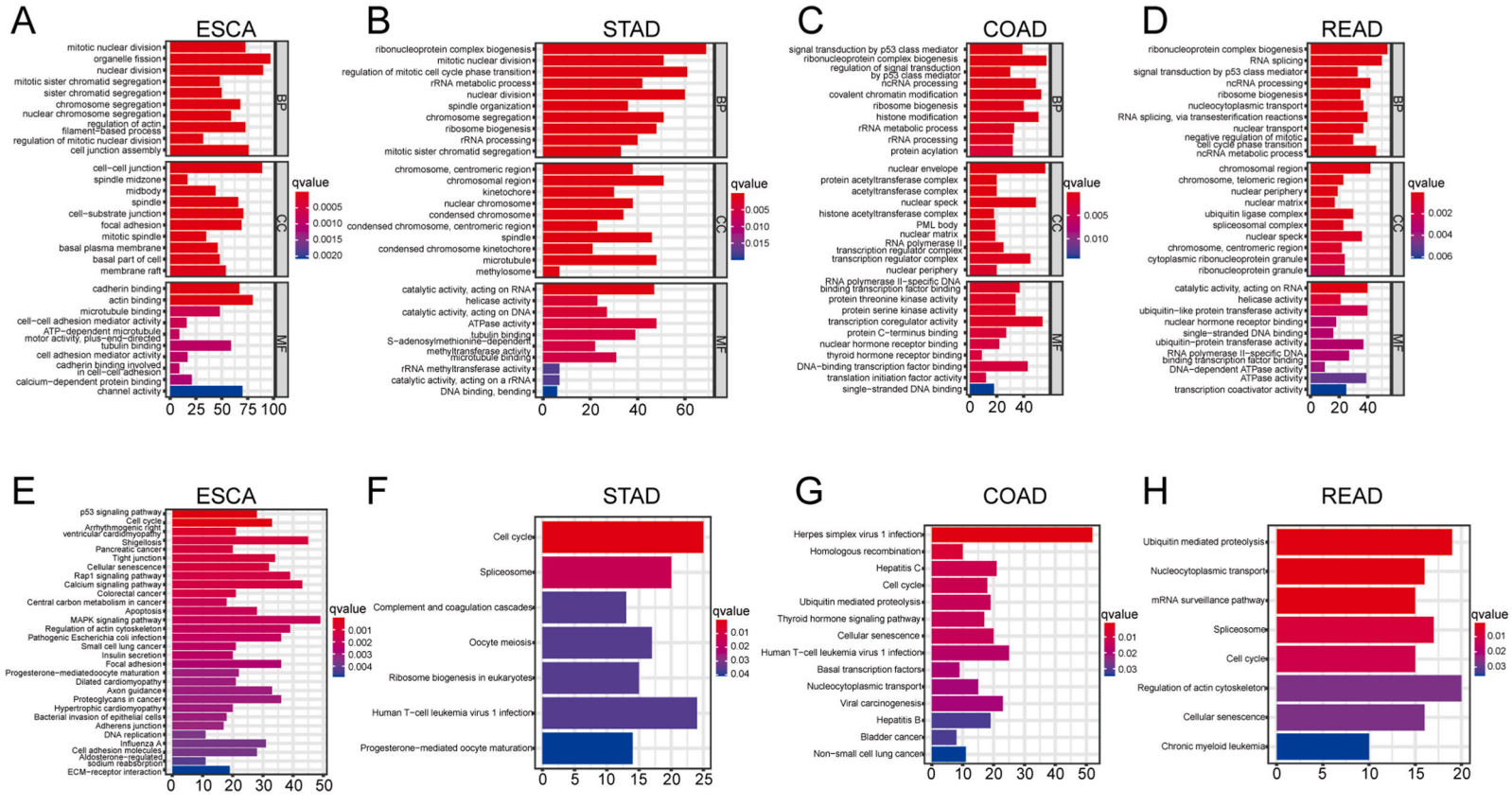

Fig. 3. Biological behaviors in distinct m6A modification patterns. (A–D) GO analysis of differential genes enrichment between m6A clusters in ESCA, STAD, COAD and READ. (E–H) KEGG analysis of differential genes in distinct m6A modification patterns of ESCA, STAD, COAD and READ.

"erasers", FTO and ALKBH5 both exhibited low mutation frequencies, where the mutation rate of ALKBH5 was less frequent than that of FTO. HNRNPC even showed no mutations in ESCA and READ patient samples. Analysis of CNV showed a widespread alteration of m6A regulators among digestive tract tumors (Fig. S1). CNV alterations were prevalent in 25 m6A genes, and most were concentrated in copy number amplification. KIAA1429 had CNV amplification in these tumors. YTHDC2 showed gained CNV in tumors except for COAD, while YTHDF1 showed gained CNV in tumors except for READ. YTHDF2 showed an extremely high frequency of CNV deletion among these four tumor types. ELAVL1, ALKBH5, RBM15, RBM15B and YTHDC2 also exhibited the same tendency. The widespread frequency of somatic mutations and CNV alterations could be prominent factors leading to dysregulation of m6A regulators expression.

The interactions and correlations among these regulators and their clinical prognostic significance to patients were analyzed (Fig. 1I-L). A positive correlation was observed among most regulators, except the correlation between FTO and IGF2BP2 in STAD and the correlation between ALKBH5 and half of the regulators in COAD. Not only did m6A regulators of the same functional class but also the function of mutual exclusion between "writers" and "eraser" showed a significant positive correlation, which confirmed that the regulation of m6A regulators is dynamically equilibrium. Most "writers" and "readers" acted as risk factors in ESCA. YTHDF1-3 and YTHDC1-2 were correlated with favorable outcomes, while IGF2BP1-3 was correlated with poor outcomes in STAD. FTO and ALKBH5 were both correlated with poor outcomes in COAD. In READ, most regulators were favorable factors.

3.2. Consensus cluster of m6A regulators based on their expression pattern

Based on the GEO and TCGA cohort, consensus unsupervised clustering analysis was used to divided patients into several m6A modification patterns. After comparing the increased area under the delta curve, $k = 3$ was demonstrated to be the most appropriate choice for dividing the patient population of ESCA, STAD and COAD into three clusters (Fig. S2A-C), and $k = 4$ was shown to be the most convenient selection for patients in READ cohort (Fig. S2D). We referred to these patterns as cluster A-D (Fig. S2E-H). Among these different m6A clusters, there was a clear distinction in the transcriptional expression data of m6A regulators (Fig. 2A–D). In ESCA, cluster A presented variable decreases in IGF2BP1-3; cluster B showed increased expression of m6A readers compared to cluster A; and cluster C exhibited increases in expression of all regulators, especially IGF2BP1-3 (Fig. 2A). The results indicated that IGF2BPs might play a functional role in patients with ESCA.

Survival analysis revealed the worst outcome of the cluster C modification pattern in ESCA (Fig. 2E). However, cluster A, with decreased expression of IGF2BP1-3 revealed a prominent survival advantage in STAD (Fig. 2F). Cluster C in COAD and cluster D in READ were both characterized by almost all-decreased expression of m6A regulators and showed the worst outcome in survival analysis (Fig. 2G and H).

3.3. Enrichment analysis of distinct m6A modification patterns

Gene set variation analysis (GSVA) was conducted to analyze the different enrichment of biological behaviors among the different m6A clusters [21]. Metabolism enrichment was outstanding in these results (Fig. S3-S6). As displayed in Fig. S3A, cluster A in ESCA was markedly enriched in autoimmune thyroid disease, tryptophan metabolism, histidine metabolism, fatty acid metabolism, butanoate metabolism, oxidative phosphorylation, lipid metabolism, linolenic acid metabolism, arachidonic acid metabolism, retinol metabolism and sucrose metabolism. Cluster B was primarily related to DNA replication, the cell cycle, primary bile acid biosynthesis, glycosaminoglycan degradation, glycan biosynthesis and retinol metabolism (Fig. S3B). Cluster C was associated with pyrimidine metabolism, cysteine and methionine metabolism and RNA degradation (Fig. S3C). In addition, clusters of m6A with poor prognosis in ESCA and STAD show enrichment of pathways associated with DNA damage response, such as proteasome, homologous recombination, mismatch repair, and spliceosome. However, in COAD and READ, m6A clusters with poor prognosis was markedly enriched in reprogramming of carbohydrate metabolism. These results demonstrate remarkable metabolic heterogeneity between tumor types. Metabolic reprogramming may result from diverse somatic driver alterations in different tumor contexts [20]. Dysregulation of m6A regulation patterns could contribute to cancer cells accumulating metabolic alterations.

To further investigate the biological function of each m6A modification pattern, we overlapped common DEGs between clusters. The limma R package was applied to distinguish DEGs and the clusterProfiler package was used for classification and enrichment analysis of DEGs. Although the metabolic pattern between m6A clusters is heterogeneous in different tumor types, we found that the pathways and functional effects of differential genes enrichment between m6A clusters were strongly consistent in different types of digestive tract tumors. GO analysis showed enrichment of biological processes associated with cell cycles, such as nuclear division, mitosis (Fig. 3A–D). KEGG analysis showed enrichment of pathways associated with cell proliferation, such as cell cycle, p53 signaling pathway, cellular senescence (Fig. 3E–H). The results imply that m6A modifications in tumor cells probably drive metabolic reprogramming to sustain rapid proliferation of cancer cells.

Collectively, m6A dysregulation and metabolic reprogramming are inherently coupled in tumors. Although there is heterogeneity in m6A patterns and metabolic alterations in different types of tumors, functional effects of m6A modification dysregulation enrichment at common pathways. Therefore, these m6A regulators may be a class of therapeutic targets to prevent metabolic disorders and tumor progression.

3.4. Association between m6A clusters and seven kinds of metabolism

The above dates demonstrate that m6A modification patterns characterize tumor metabolic heterogeneity and progression. To further confirm the correlation between m6A clusters and metabolic characteristics in these four tumors, we curated seven metabolic

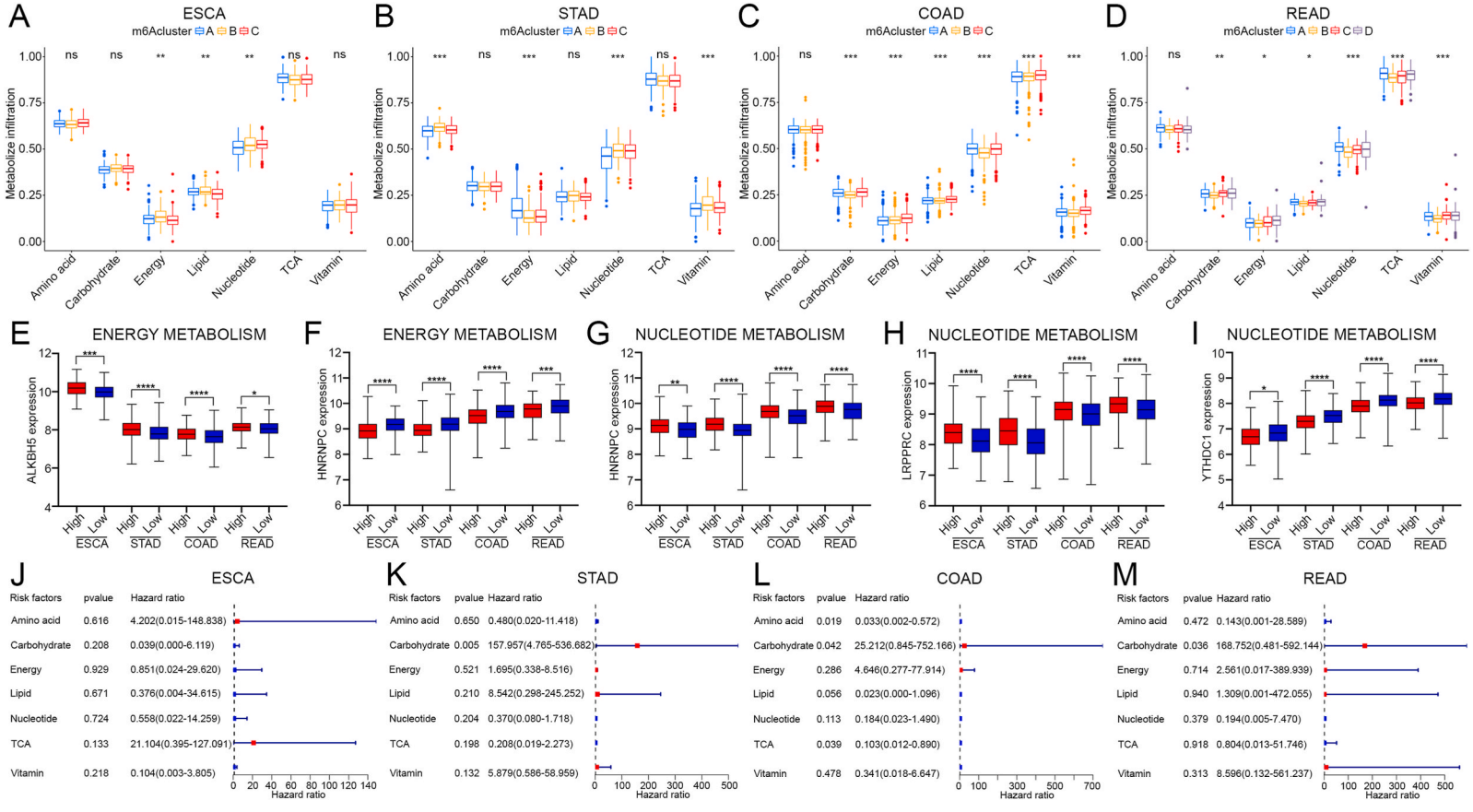

Fig. 4. Role of metabolism in different m6A clusters. (A–D) Abundance of each metabolism in the several m6A modification patterns in ESCA, STAD, COAD and READ. The upper and lower ends of the boxes represent the interquartile distance of the values. Lines in the boxes represent median values and dots represent outliers. Asterisks represent statistical p-values ($P < 0.001$, '***', $P < 0.01$ '**', $P < 0.05$ '*') (E) Expression of ALKBH5 in high and low expression group of energy metabolism. (F) Expression of HNRNPC in high and low expression group of energy metabolism. (G) Expression of HNRNPC in high and low expression group of nucleotide metabolism. (H) Expression of LRPPRC in high and low expression group of nucleotide metabolism. (I) Expression of YTHDC1 in high and low expression group of nucleotide metabolism. (J–M) Univariate analysis of seven kinds of metabolisms to identify the metabolism that significantly correlated with OS in ESCA, STAD, COAD and READ.

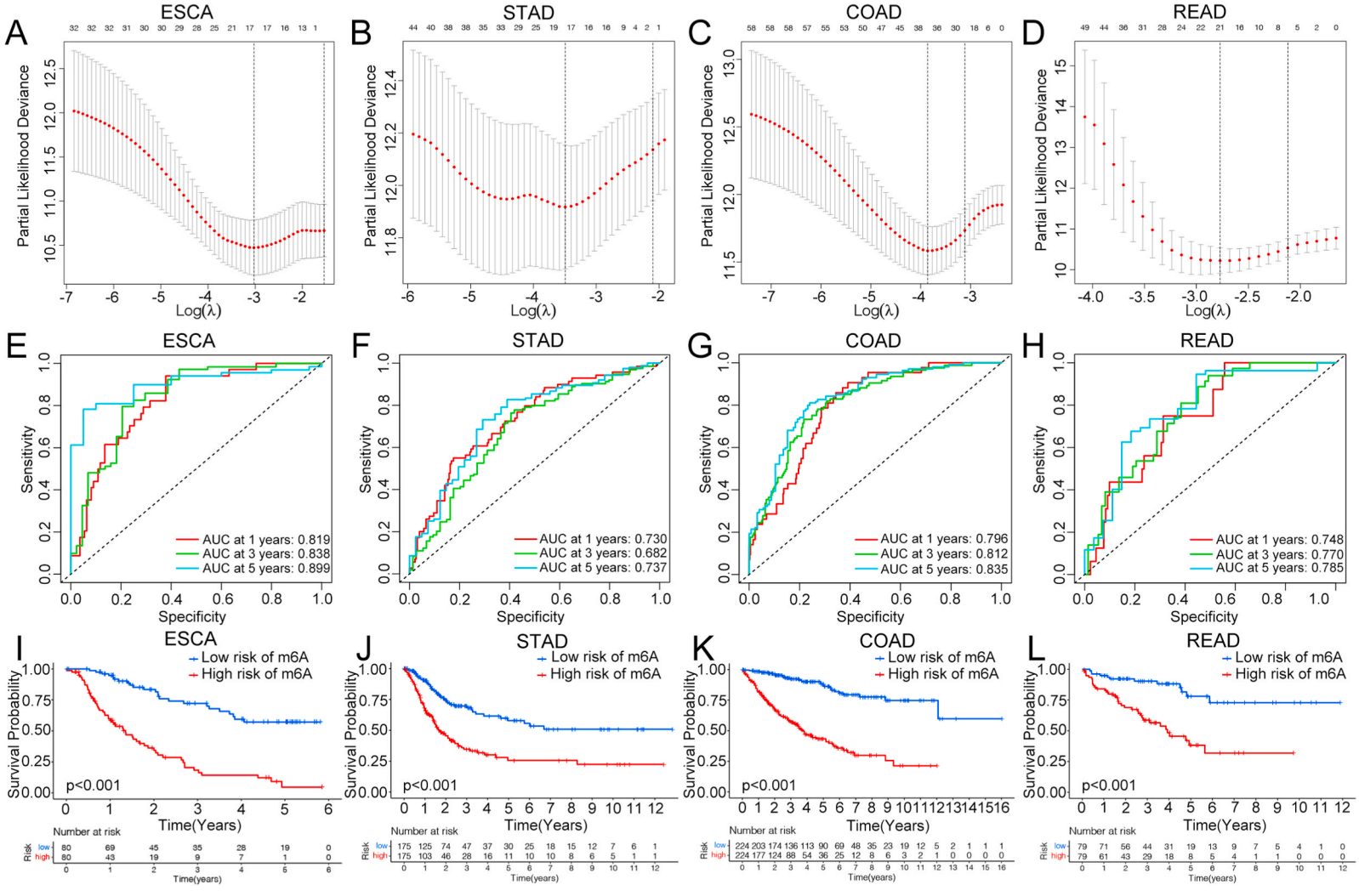

Fig. 5. Construction of the prognostic signature of m6A risk. (A–D) The prognostic signature of m6A risk constructed by the minimum criterion of LASSO Cox regression algorithm in ESCA, STAD, COAD and READ. (E–H) Time-dependent ROC curves for risk models. Results of test sets were shown in four kinds of tumors. (I–L) Survival analysis of risk models. Construction of survival curves for the test set by Kaplan-Meier analysis in ESCA, STAD, COAD and READ.

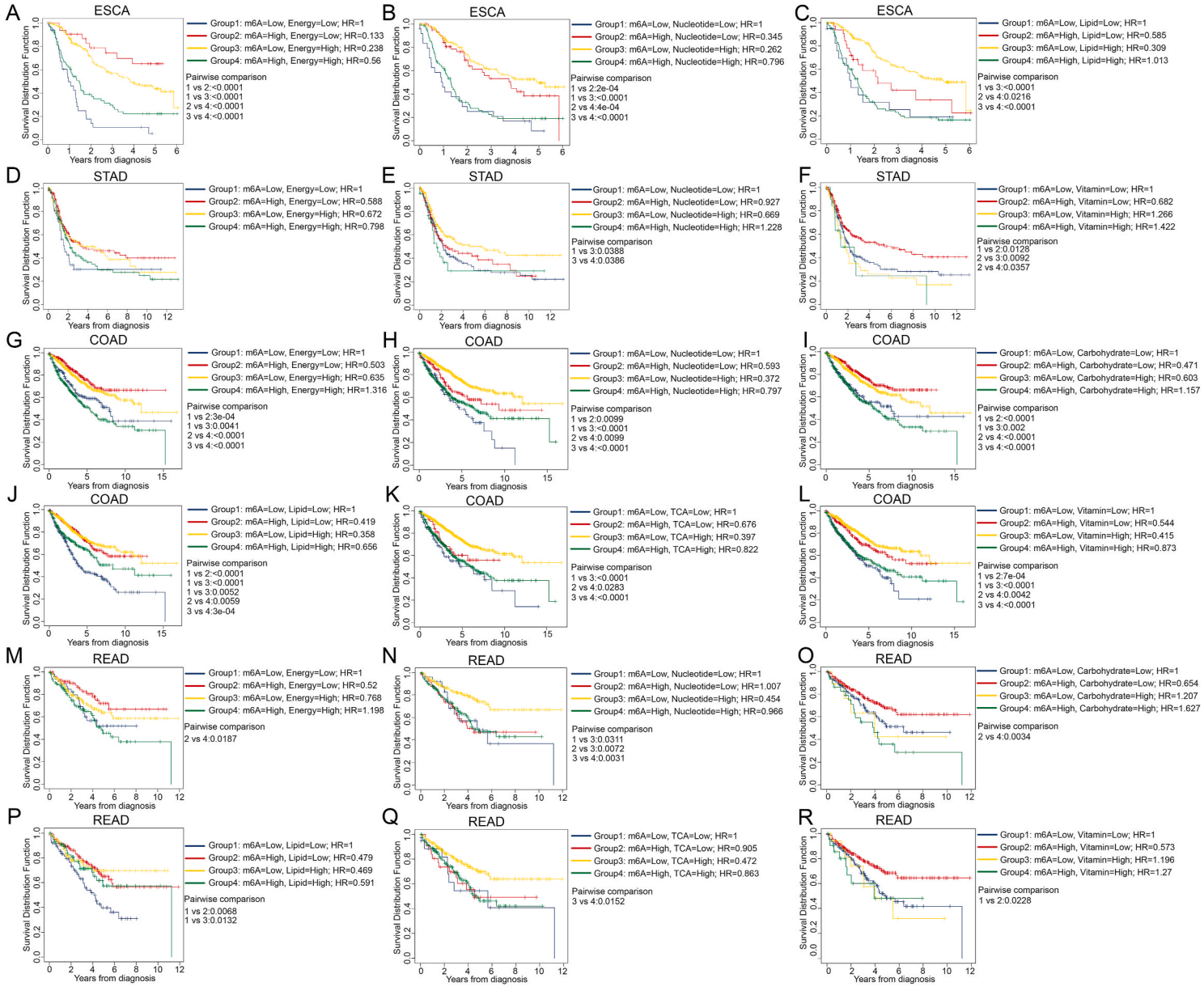
A
ESCA
Survival Distribution Function
Years from diagnosis
Group1: m6A=Low, Energy=Low; HR=1
Group2: m6A=High, Energy=Low; HR=0.133
Group3: m6A=Low, Energy=High; HR=0.238
Group4: m6A=High, Energy=High; HR=0.56
Pairwise comparison
1 vs 2:<0.0001
1 vs 3:<0.0001
2 vs 4:<0.0001
3 vs 4:<0.0001
B
ESCA
Group1: m6A=Low, Nucleotide=Low; HR=1
Group2: m6A=High, Nucleotide=Low; HR=0.345
Group3: m6A=Low, Nucleotide=High; HR=0.262
Group4: m6A=High, Nucleotide=High; HR=0.796
Pairwise comparison
1 vs 2:2e-04
1 vs 3:<0.0001
2 vs 4:4e-04
3 vs 4:<0.0001
C
ESCA
Group1: m6A=Low, Lipid=Low; HR=1
Group2: m6A=High, Lipid=Low; HR=0.585
Group3: m6A=Low, Lipid=High; HR=0.309
Group4: m6A=High, Lipid=High; HR=1.013
Pairwise comparison
1 vs 3:<0.0001
2 vs 4:0.0216
3 vs 4:<0.0001
D
STAD
Group1: m6A=Low, Energy=Low; HR=1
Group2: m6A=High, Energy=Low; HR=0.588
Group3: m6A=Low, Energy=High; HR=0.672
Group4: m6A=High, Energy=High; HR=0.798
E
STAD
Group1: m6A=Low, Nucleotide=Low; HR=1
Group2: m6A=High, Nucleotide=Low; HR=0.927
Group3: m6A=Low, Nucleotide=High; HR=0.669
Group4: m6A=High, Nucleotide=High; HR=1.228
Pairwise comparison
1 vs 3:0.0388
3 vs 4:0.0386
F
STAD
Group1: m6A=Low, Vitamin=Low; HR=1
Group2: m6A=High, Vitamin=Low; HR=0.682
Group3: m6A=Low, Vitamin=High; HR=1.266
Group4: m6A=High, Vitamin=High; HR=1.422
Pairwise comparison
1 vs 2:0.0128
2 vs 3:0.0092
2 vs 4:0.0357
G
COAD
Group1: m6A=Low, Energy=Low; HR=1
Group2: m6A=High, Energy=Low; HR=0.503
Group3: m6A=Low, Energy=High; HR=0.635
Group4: m6A=High, Energy=High; HR=1.316
Pairwise comparison
1 vs 2:3e-04
1 vs 3:0.0041
2 vs 4:<0.0001
3 vs 4:<0.0001
H
COAD
Group1: m6A=Low, Nucleotide=Low; HR=1
Group2: m6A=High, Nucleotide=Low; HR=0.593
Group3: m6A=Low, Nucleotide=High; HR=0.372
Group4: m6A=High, Nucleotide=High; HR=0.797
Pairwise comparison
1 vs 2:0.0099
1 vs 3:<0.0001
2 vs 4:0.0099
3 vs 4:<0.0001
I
COAD
Group1: m6A=Low, Carbohydrate=Low; HR=1
Group2: m6A=High, Carbohydrate=Low; HR=0.471
Group3: m6A=Low, Carbohydrate=High; HR=0.603
Group4: m6A=High, Carbohydrate=High; HR=1.157
Pairwise comparison
1 vs 2:<0.0001
1 vs 3:0.002
2 vs 4:<0.0001
3 vs 4:<0.0001
J
COAD
Group1: m6A=Low, Lipid=Low; HR=1
Group2: m6A=High, Lipid=Low; HR=0.419
Group3: m6A=Low, Lipid=High; HR=0.358
Group4: m6A=High, Lipid=High; HR=0.656
Pairwise comparison
1 vs 2:<0.0001
1 vs 3:<0.0001
1 vs 3:0.0052
2 vs 4:0.0059
3 vs 4:3e-04
K
COAD
Group1: m6A=Low, TCA=Low; HR=1
Group2: m6A=High, TCA=Low; HR=0.676
Group3: m6A=Low, TCA=High; HR=0.397
Group4: m6A=High, TCA=High; HR=0.822
Pairwise comparison
1 vs 3:<0.0001
2 vs 4:0.0283
3 vs 4:<0.0001
L
COAD
Group1: m6A=Low, Vitamin=Low; HR=1
Group2: m6A=High, Vitamin=Low; HR=0.544
Group3: m6A=Low, Vitamin=High; HR=0.415
Group4: m6A=High, Vitamin=High; HR=0.873
Pairwise comparison
1 vs 2:7e-04
1 vs 3:<0.0001
2 vs 4:0.0042
3 vs 4:<0.0001
M
READ
Group1: m6A=Low, Energy=Low; HR=1
Group2: m6A=High, Energy=Low; HR=0.52
Group3: m6A=Low, Energy=High; HR=0.768
Group4: m6A=High, Energy=High; HR=1.198
Pairwise comparison
2 vs 4:0.0187
N
READ
Group1: m6A=Low, Nucleotide=Low; HR=1
Group2: m6A=High, Nucleotide=Low; HR=1.007
Group3: m6A=Low, Nucleotide=High; HR=0.454
Group4: m6A=High, Nucleotide=High; HR=0.966
Pairwise comparison
1 vs 3:0.0311
2 vs 3:0.0072
3 vs 4:0.0031
O
READ
Group1: m6A=Low, Carbohydrate=Low; HR=1
Group2: m6A=High, Carbohydrate=Low; HR=0.654
Group3: m6A=Low, Carbohydrate=High; HR=1.207
Group4: m6A=High, Carbohydrate=High; HR=1.627
Pairwise comparison
2 vs 4:0.0034
P
READ
Group1: m6A=Low, Lipid=Low; HR=1
Group2: m6A=High, Lipid=Low; HR=0.479
Group3: m6A=Low, Lipid=High; HR=0.469
Group4: m6A=High, Lipid=High; HR=0.591
Pairwise comparison
1 vs 2:0.0068
1 vs 3:0.0132
Q
READ
Group1: m6A=Low, TCA=Low; HR=1
Group2: m6A=High, TCA=Low; HR=0.905
Group3: m6A=Low, TCA=High; HR=0.472
Group4: m6A=High, TCA=High; HR=0.863
Pairwise comparison
3 vs 4:0.0152
R
READ
Group1: m6A=Low, Vitamin=Low; HR=1
Group2: m6A=High, Vitamin=Low; HR=0.573
Group3: m6A=Low, Vitamin=High; HR=1.196
Group4: m6A=High, Vitamin=High; HR=1.27
Pairwise comparison
1 vs 2:0.0228

Fig. 6. Survival analysis were assessed bifactorally using m6A scores and seven metabolisms. (A–C) Metabolism type which showed significance among m6A clusters were chose to be showed in ESCA. (D–F) Metabolism type which showed significance among m6A clusters were chose to be showed in STAD. (G–L) Metabolism type which showed significance among m6A clusters were chose to be showed in COAD. (M–R) Metabolism type which showed significance among m6A clusters were chose to be showed in READ. The results were compared two by two according to the four cases in the lower left corner, and the P values of the compared results were in the upper right corner, and only $P < 0.05$ results were retained.

super-pathways gene sets whose expression patterns were confirmed to reflect actual metabolic activities in cancer patients [20]. ssGSEA analysis was used to calculate the enrichment fraction of metabolism in patient sample (Fig. 4A–D). One-way ANOVA analysis showed that these m6A modification clusters showed common distinct differences between energy metabolism and nucleotide metabolism among the four kinds of tumors. Lipid metabolism exhibited overlaps in tumors except STAD (Fig. 4B), while vitamin metabolism exhibited infiltration in tumors except ESCA (Fig. 4B–D). Amino acid metabolism only showed significant infiltration in STAD (Fig. 4B). The clusters also had significant infiltration of carbohydrate metabolism and TCA metabolism in COAD and READ (Fig. 4C and D). This finding further emphasizes that m6A modification act a pivotal part in tumor metabolic reprogramming.

High and low expression groups of patients were distinguished according to the median metabolism enrichment fraction. Expression of m6A regulators were also compared (Fig. 4E–I, Fig. S7). Surprisingly, we found that ALKBH5 showed a high enrichment in high-score energy metabolism group of these four kinds of tumors (Fig. 4E), while HNRNPC showed the opposite expression (Fig. 4F). The metabolic patterns among m6A clusters are heterogeneous, but quite a few m6A regulators have consistent correlations with metabolic subtypes. These m6A regulators serve as key nodes in regulating tumor metabolic activity.

Moreover, univariate Cox regression analysis was performed to evaluate the impact of metabolism risk on patient prognosis (Fig. 4J-M). Results showed that carbohydrate metabolism acted an outstanding role in digestive tract tumors except ESCA ($p = 0.005$, $HR = 157.957$ in STAD, $p = 0.042$, $HR = 25.212$ in COAD and $p = 0.036$, $HR = 168.752$ in READ).

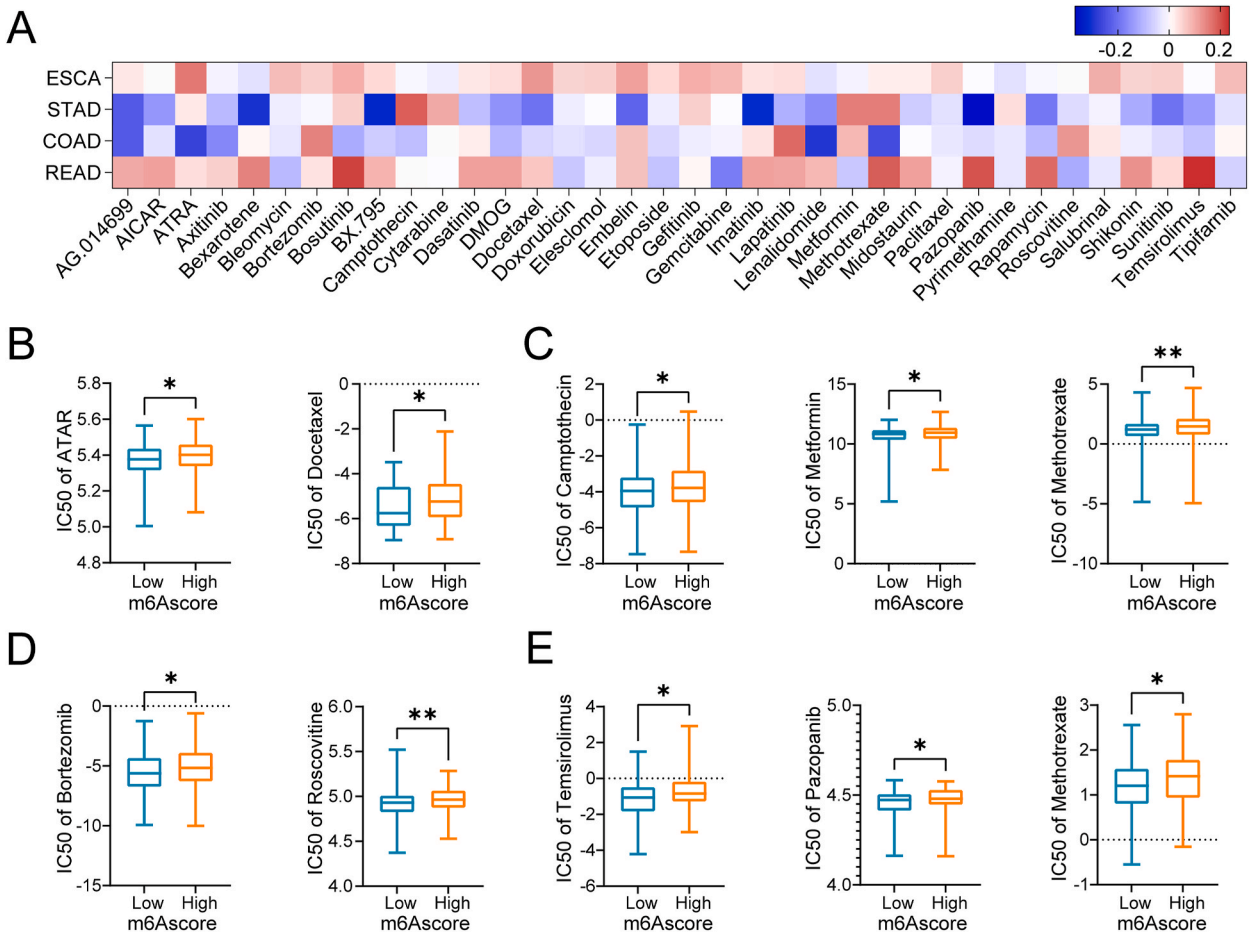

Fig. 7. Potency of the m6A risk score in predicting drug sensitivity. (A)The correlation of m6A score and IC50 values of chemotherapy drugs in four kind digestive tract tumors. (B–E) The IC50 data of drugs in high and low m6A risk score group (B), STAD (C), COAD (D) and READ (E). Asterisks represent statistical P values (*$P < 0.05$; **$P < 0.01$; ***$P < 0.001$).

3.5. Constructing m6A-related risk models

The above results showed a landscape of m6A regulators among the patient population. Taking the heterogeneity of m6A modification into account, a scoring system about m6A risk of individual patient was constructed, which we called m6A score (Fig. 5A–D). The median risk score was used to divide patients into high- and low-risk groups.

The model receiver operating characteristic (ROC) curves were predicted using the time ROC package and validated in the test set (Fig. 5E–H) and validation set (Fig. S8A-D), respectively. Through the ROC curve, we found that in the test set, areas under the curve (AUCs) were 0.819, 0.838, and 0.899 at 1, 3, and 5 years in ESCA (Fig. 5E). These results showed the specificity and sensitivity of m6A risk among digestive tract tumors. Kaplan-Meier survival analysis revealed that m6A risk score was significantly associated with survival of patients in test set and validation set. Patients in the high-risk group showed shorter survival probability ($p < 0.001$) (Fig. 5I-L, Fig. S8E-H). The results verify that m6A score is a novel and reliable prognostic biomarker for patients with digestive tract tumors.

To finally confirm the clinical significance of m6A risk and the seven kinds of metabolism in tumors, survival analysis was conducted. Surprisingly, patients who had the worst prognosis had the same score of m6A and metabolism (Fig. 6A-Q). For example, patients with low m6A scores and energy metabolism showed the worst survival rate in ESCA (Fig. 6A). One exception was the signal of low m6A scores and high vitamin cofactor metabolism scores in READ, which showed the worst prognosis (Fig. 6R). This suggested that simultaneous alterations in m6A and metabolism scores discriminate patients into different prognoses.

3.6. Potency of the m6A risk score in predicting drug sensitivity

Metabolic therapy is an extremely promising target to prevent tumor development. However, heterogeneous metabolism exists across tumor types and different evolutionary stages. To explore the value of m6A risk score in predicting drug sensitivity, R package " oncoPredict " was used to calculate sensitivity scores of drugs in the GDSC database, thereby evaluating the application of m6A risk score [22]. Results showed that a positive correlation was observed between m6A risk score and IC50 of most drugs in ESCA and READ. However, the correlation is heterogeneous in STAD and COAD (Fig. 7A). Surprisingly, we found that the IC50 of many metabolism-related drugs showed a high enrichment in high m6A risk score group. Such as, methotrexate in STAD and READ, metformin in STAD (Fig. 7B–E). These results confirm that the m6A risk score is a valuable indicator for predicting metabolic drugs sensitivity.

4. Discussion

As the incidence and mortality rates of digestive tract tumors have been increasing year by year, the study of their pathogenesis and progression has gradually attracted considerable attention [23,24]. M6A, as an important component of epigenetics, has a broad and significant influence on the regulation of gene expression in cells [6,25]. Due to technical limitations, most previous studies analyzed the role of individual m6A regulators. However, m6A modification in tumors is dynamic and reversible, and multiple m6A regulators may play synergistic or mutually exclusive roles in tumor progression [25]. Therefore, comprehensively analyzing the genetic variation and expression patterns of m6A-related regulators in digestive tract tumors, comparing their functional differences and clinical features among different clusters, and constructing a categorization system to classify their m6A risk factors can help us deeply understand the role and specific characteristics of m6A in tumors and provide new ideas for the clinical treatment of patients.

In this work, we tested and validated the expression and clinical significance of 25 m6A regulators. Our results suggest that somatic mutations and CNV alterations of the m6A regulator are prevalent in digestive tract tumors. The m6A regulators are highly heterogeneous in their genetic alterations, suggesting that they may be related to tumor evolutionary diversity. Analysis of the expression of m6A regulatory genes showed that most regulatory factors were highly expressed in tumor samples. However, some m6A regulatory factors are also expressed at different levels between tumor types. It has been suggested that there is heterogeneity in the m6A modification among tumor types. Correlation analysis showed that most of the m6A regulators were positively correlated with each other, suggesting that multiple regulators may have a combined effect on tumors. Not only do there exist significant positive correlations between m6A regulators of the same functional class, but also between genes with mutually exclusive functions of methylases and demethylases, confirming that the regulation of m6A regulators is dynamically balanced. Survival analysis showed that most m6A regulatory factors were associated with prognosis in digestive tract tumor patients. Of these, both FTO and ALKBH5 were associated with poor prognosis in COAD. However, ALKBH5 expression levels in normal tissues are significantly higher than in COAD. The possible reason for this is that we based our analysis on mRNA levels, while other factors such as post-transcriptional mechanisms may also influence the effect of ALKBH5 on COAD prognosis. The role of ALKBH5 in COAD reported in the literature is also controversial [26–28]. Therefore, further experimental studies are required to confirm it.

We quantified and clustered the expression patterns of the m6A regulator in patients with digestive tract tumors in the TCGA cohort. M6A clusters with increased expression of IGF2BPs showed the worst outcomes in STAD and ESCA. Indeed, previous studies have showed that the reader and especially the IGF2BPs were upregulated in cancers, patients with a high IGF2BPs signature exhibited poor prognosis across cancer types [29–31]. However, the clusters in COAD and READ characterized by nearly all m6A regulators with reduced expression showed the best results in the survival analysis. The M6A regulator has the ability to target hundreds of M6A-modified transcripts, including oncogenes and antioncogenes [7,26]. Moreover, the ultimate fate of m6A-modified mRNAs critically depends on the m6A reader [32,33]. We have analyzed the combined effects of all m6A regulators in COAD and READ, and cannot rule out the oncogenic effects of individual m6A regulators in COAD and READ.

Metabolic reprogramming is an important factor in tumor development [15,16,20]. Interestingly, functional enrichment analysis across different clusters suggests that m6A regulators are closely related to metabolism. Reprogramming of carbohydrate metabolism has already occurred at the precancerous adenoma stage [14]. Our results also suggest that in CRCs, the m6A clusters with poor prognosis are significantly enriched in reprogrammed carbohydrate metabolism. Based on our findings, both energy metabolism and nucleotide metabolism are different in m6A clusters in digestive tract tumors, suggesting a potential therapeutic target for metabolic therapy. TCA metabolism is also localized at a higher level of overlap than other metabolic types, and shows significance among the m6A clusters in COAD and READ. Analyzing the biological functions of DEGs between each m6A cluster, enrichment analysis revealed that although the metabolic patterns between m6A clusters in different types of tumors were heterogeneous, there was a strong consistency in the pathways and functions of differentially enriched genes between m6A clusters in different types of digestive tract tumors. Biological processes related to the cell cycle and pathways associated with cell proliferation are significantly enriched. These results suggest that m6A modifications in tumor cells may drive metabolic reprogramming to sustain the rapid proliferation of cancer cells. The expression patterns of gene sets of metabolic pathways have been shown to reflect the actual metabolic profile of cancer patients [20]. Our analysis based on gene sets of metabolic pathways also shows that both energy metabolism and nucleotide metabolism exhibit significant differences among m6A clusters in digestive tract tumors. However, other metabolic pathways show heterogeneity across tumor types. In addition, a comparison of m6A regulator expression based on various metabolic enrichment scores also showed that multiple m6A regulators exhibited higher enrichment in the high-energy metabolism groups of these four tumor types. The relationship of m6A and tumor metabolism has been reported [18,34]. Through systematic analysis, we demonstrate significant metabolic heterogeneity between tumor types, with the m6A cluster being able to characterize metabolic phenotypes well.

Metabolic reprogramming has already altered at early stages of carcinogenesis, suggesting that metabolism may be a target for early prediction of cancer recurrence and treatment response [14,35]. Metabolic therapies are currently achieving remarkable results in inhibiting the malignant progression of tumors [36]. However, clinical trials have shown that only certain tumors respond well to metabolic therapy. To identify this group of metabolically susceptible tumors, there is an urgent need to identify subgroups of patients who respond differently to metabolic therapy. Thus, we constructed a scoring system about m6A risk, called as m6A score. The M6A score can be used as a common screening metric to provide a significant distinction in patient prognosis. The m6A score and metabolic score of the patients with the worst prognosis were consistent. This suggests that the m6A score is a new and reliable prognostic marker for predicting the metabolic characteristics of digestive tract tumors and patient outcome. In addition, we found that many metabolism-related drugs showed higher IC50 levels in groups with high m6A scores. Examples are methotrexate in STAD and READ, and metformin in STAD. Although therapies targeting multiple metabolic pathways have been shown to be effective in suppressing tumor malignant phenotypes, they are still less frequently used in clinical practice, with the greatest difficulty being the heterogeneity of tumor metabolism and the lack of sensitive biomarkers to predict the effect of metabolic therapy [16,20,37]. In our study, the m6A score was positively correlated with the IC50 of metabolism-related drugs such as methotrexate and metformin, suggesting that patients with high m6A scores were poorly treated with these drugs. The association of methotrexate and metformin with m6A modification and their role in preclinical anti-tumor has been reported [38–40], but their clinical effects require further confirmation. The results of the present study suggest that the m6A score is a very promising predictor of metabolic drug sensitivity. It provides a theoretical basis for clinical treatment regimens.

There are some limitations of this study. First, mRNAs were analyzed without protein-level analysis. The post-transcriptional mechanism of the M6A regulator may also lead to changes in the m6A modifications, resulting in heterogeneity. Second, mechanistic analysis and further experimental confirmation are difficult to perform because this study is a comprehensive analysis of the changes in the m6A regulator in digestive tract tumors and elaborates on the results of their combined effects. Third, the present study is based on limited information obtained from cancer profiles and cannot rule out the influence of other factors on the conclusions. Finally, due to metabolic heterogeneity, most current studies are preclinical explorations, limiting our ability to further analyze the evaluation of m6A modifications with metabolic therapeutic effects. Further testing based on more clinical samples may provide additional support. Despite these limitations, a number of small-molecule inhibitors targeting m6A regulators have been demonstrated to have promising antitumor effects in preclinical studies [41,42]. Thus, the m6A modification pattern has the potential to guide or improve metabolic therapies.

In conclusion, we have successfully demonstrated the role of m6A and its regulators in digestive tract tumors, providing new insight into the relevance of m6A to metabolism. Understanding these m6A- and metabolism-related features provides a new strategy for future metabolic therapy and prognosis determination in digestive tract tumors.

Ethics approval and consent to participate

Not applicable.

Funding

This work was supported by the National Natural Science Foundation of China, China (No. 82372756); Natural Science Foundation of Chongqing, China (No. cstc2020jcyj-zdxmX0020).

CRediT authorship contribution statement

Bing He: Conceptualization, Data Curation; Yiyang Hu: Conceptualization, Writing-Original Draft; Hui Chen: Investigation,

Visualization; Xia Xie: Funding acquisition, Supervision; Chunli Gong: Resources, Investigation; Li Zhibin: Methodology, Validation; Yang Chen: Software, Formal analysis; Yufeng Xiao: Conceptualization, Supervision; Shiming Yang: Conceptualization, Project administration.

Data availability statement

The results presented in our study are based on data generated from the TCGA and GEO databases. All data used in this study can be downloaded from TCGA (https://gdc.cancer.gov) and GEO (https://www.ncbi.nlm.nih.gov/geo).

Declaration of competing interest

The authors declare that they have no known competing financial interests or personal relationships that could have appeared to influence the work reported in this paper.

Acknowledgments

We sincerely appreciate all lab members.

Appendix A. Supplementary data

Supplementary data related to this article can be found at https://doi.org/10.1016/j.heliyon.2024.e24235.

References

[1] F. Bray, J. Ferlay, I. Soerjomataram, R.L. Siegel, L.A. Torre, A. Jemal, Global cancer statistics 2018: GLOBOCAN estimates of incidence and mortality worldwide for 36 cancers in 185 countries, CA Cancer J Clin 68 (6) (2018) 394–424, https://doi.org/10.3322/caac.21492.
[2] L. Gu, Y. Liu, C. Jiang, L. Sun, H. Zhou, Identification and clinical validation of metastasis-associated biomarkers based on large-scale samples in colon-adenocarcinoma, Pharmacol. Res. 160 (2020) 105087, https://doi.org/10.1016/j.phrs.2020.105087.
[3] D. Zang, C. Zhang, C. Li, et al., LPPR4 promotes peritoneal metastasis via Sp1/integrin alpha/FAK signaling in gastric cancer, Am. J. Cancer Res. 10 (3) (2020) 1026–1044, eCollection 2020.
[4] Y. Kawaguchi, J.N. Vauthey, The landmark series: randomized control trials examining perioperative chemotherapy and postoperative adjuvant chemotherapy for resectable colorectal liver metastasis, Ann. Surg Oncol. 27 (11) (2020) 4263–4270, https://doi.org/10.1245/s10434-020-08777-z.
[5] S. St James, B. Bednarz, S. Benedict, et al., Current status of radiopharmaceutical therapy, Int. J. Radiat. Oncol. Biol. Phys. 109 (4) (2021) 891–901, https://doi.org/10.1016/j.ijrobp.2020.08.035.
[6] D. Dominissini, S. Moshitch-Moshkovitz, S. Schwartz, et al., Topology of the human and mouse m6A RNA methylomes revealed by m6A-seq, Nature 485 (7397) (2012) 201–206, https://doi.org/10.1038/nature11112.
[7] Z. Li, H. Weng, R. Su, et al., FTO plays an oncogenic role in acute myeloid leukemia as a N(6)-methyladenosine RNA demethylase, Cancer Cell 31 (1) (2017) 127–141, https://doi.org/10.1016/j.ccell.2016.11.017.
[8] R. Su, L. Dong, C. Li, et al., R-2HG exhibits anti-tumor activity by targeting FTO/m(6)A/MYC/CEBPA signaling, Cell 172 (1–2) (2018) 90–105, https://doi.org/10.1016/j.cell.2017.11.031, e123.
[9] Y. Pan, K. Xiao, Y. Li, Y. Li, Q. Liu, RNA N6-methyladenosine regulator-mediated methylation modifications pattern and immune infiltration features in glioblastoma, Front. Oncol. 11 (2021), https://doi.org/10.3389/fonc.2021.632934.
[10] Z. Yang, T. Wang, D. Wu, Z. Min, J. Tan, B. Yu, RNA N6-methyladenosine reader IGF2BP3 regulates cell cycle and angiogenesis in colon cancer, J. Exp. Clin. Cancer Res. 39 (1) (2020) 203, https://doi.org/10.1186/s13046-020-01714-8.
[11] H. Guo, B. Wang, K. Xu, et al., m(6)A reader HNRNPA2B1 promotes esophageal cancer progression via up-regulation of ACLY and ACC1, Front. Oncol. 10 (2020), https://doi.org/10.3389/fonc.2020.553045.
[12] Q. Yao, L. He, X. Gao, et al., The m6A methyltransferase METTL14-mediated N6-methyladenosine modification of PTEN mRNA inhibits tumor growth and metastasis in stomach adenocarcinoma, Front. Oncol. 11 (2021), https://doi.org/10.3389/fonc.2021.699749.
[13] C. Cai, J. Long, Q. Huang, et al., M6A "writer" gene METTL14: a favorable prognostic biomarker and correlated with immune infiltrates in rectal cancer, Front. Oncol. 11 (2021), https://doi.org/10.3389/fonc.2021.615296.
[14] J. Li, R. Wang, X. Zhou, et al., Genomic and transcriptomic profiling of carcinogenesis in patients with familial adenomatous polyposis, Gut 69 (7) (2020) 1283–1293. https://doi:10.1136/gutjnl-2019-319438.
[15] Y. Gong, P. Ji, Y.-S. Yang, et al., Metabolic-pathway-based subtyping of triple-negative breast cancer reveals potential therapeutic targets, Cell Metabol. 33 (1) (2021) 51–64.e9. https://doi:10.1016/j.cmet.2020.10.012.
[16] B. Faubert, A. Solmonson, R.J. DeBerardinis, Metabolic reprogramming and cancer progression, Science 368 (6487) (2020), https://doi.org/10.1126/science.aaw5473.
[17] H. Weng, F. Huang, Z. Yu, et al., The m6A reader IGF2BP2 regulates glutamine metabolism and represents a therapeutic target in acute myeloid leukemia, Cancer Cell 40 (12) (2022) 1566–1582. https://doi:10.1016/j.ccell.2022.10.004.
[18] H. Chen, S. Gao, W. Liu, et al., RNA N(6)-methyladenosine methyltransferase METTL3 facilitates colorectal cancer by activating the m(6)A-GLUT1-mTORC1 Axis and is a therapeutic target, Gastroenterology 160 (4) (2021) 1284–1300, e16, https://doi:10.1053/j.gastro.2020.11.013.
[19] G. Yu, L.G. Wang, Y. Han, Q.Y. He, clusterProfiler: an R package for comparing biological themes among gene clusters, OMICS 16 (5) (2012) 284–287. https://doi:10.1089/omi.2011.0118.
[20] X. Peng, Z. Chen, F. Farshidfar, et al., Molecular characterization and clinical relevance of metabolic expression subtypes in human cancers, Cell Rep. 23 (1) (2018) 255–269 e4. https://doi:10.1016/j.celrep.2018.03.077.
[21] S. Hanzelmann, R. Castelo, J. Guinney, GSVA: gene set variation analysis for microarray and RNA-seq data, BMC Bioinf. 14 (2013) 7. https://doi:10.1186/1471-2105-14-7.
[22] D. Maeser, R.F. Gruener, R.S. Huang, oncoPredict: an R package for predicting in vivo or cancer patient drug response and biomarkers from cell line screening data, Briefings Bioinf. 22 (6) (2021) bbab260. https://doi:10.1092/bib/bbab260.

[23] J. Huang, D.E. Lucero-Prisno, L. Zhang, et al., Updated epidemiology of gastrointestinal cancers in East Asia, Nat. Rev. Gastroenterol. Hepatol. 20 (5) (2023) 271–287. https://doi:10.1038/s41575-022-00726-3.
[24] E. Morgan, M. Arnold, M.C. Camargo, et al., The current and future incidence and mortality of gastric cancer in 185 countries, 2020-40: a population-based modelling study, EClinicalMedicine 47 (2022), https://doi.org/10.1016/j.eclinm.2022.101404.
[25] Y. Li, J. Xiao, J. Bai, et al., Molecular characterization and clinical relevance of m(6)A regulators across 33 cancer types, Mol. Cancer 18 (1) (2019) 137. https://doi:10.1186/s12943-019-1066-3.
[26] J. Zhai, H. Chen, C.C. Wong, et al., ALKBH5 drives immune suppression via targeting AXIN2 to promote colorectal cancer and is a target for boosting immunotherapy, Gastroenterology 165 (2) (2023) 445–462. https://doi:10.1053/j.gastro.2023.04.032.
[27] J. Ge, S.-L. Liu, J.-X. Zheng, et al., RNA demethylase ALKBH5 suppresses tumorigenesis via inhibiting proliferation and invasion and promoting CD8+ T cell infiltration in colorectal cancer, Translational Oncology 34 (2023), https://doi.org/10.1016/j.tranon.2023.101683.
[28] M. Ye, C. Hu, T. Chen, et al., FABP5 suppresses colorectal cancer progression via mTOR-mediated autophagy by decreasing FASN expression, Int. J. Biol. Sci. 19 (10) (2023) 3115–3127. https://doi:10.7150/ijbs.85285.
[29] J. Oh, C. Hwa, D. Jang, et al., Augmentation of the RNA m6A reader signature is associated with poor survival by enhancing cell proliferation and EMT across cancer types, Exp. Mol. Med. 54 (7) (2022) 906–921. https://doi:10.1038/s12276-022-00795-z.
[30] S. Kendzia, S. Franke, T. Kröhler, et al., A combined computational and functional approach identifies IGF2BP2 as a driver of chemoresistance in a wide array of pre-clinical models of colorectal cancer, Mol. Cancer 22 (1) (2023) 89. https://doi:10.1186/s12943-023-01787-x.
[31] H. Huang, H. Weng, W. Sun, et al., Recognition of RNA N6-methyladenosine by IGF2BP proteins enhances mRNA stability and translation, Nat. Cell Biol. 20 (3) (2018) 285–295. https://doi:10.1038/s41556-018-0045-z.
[32] L. Wang, X. Dou, S. Chen, et al., YTHDF2 inhibition potentiates radiotherapy antitumor efficacy, Cancer Cell 41 (7) (2023) 1294–1308. https://doi:10.1016/j.ccell.2023.04.019.
[33] L. Wang, L. Zhu, C. Liang, et al., Targeting N6-methyladenosine reader YTHDF1 with siRNA boosts antitumor immunity in NASH-HCC by inhibiting EZH2-IL-6 axis, J. Hepatol. 79 (5) (2023) 1185–1200. https://doi:10.1016/j.jhep.2023.06.021.
[34] Q. Wang, C. Chen, Q. Ding, et al., METTL3-mediated m(6)A modification of HDGF mRNA promotes gastric cancer progression and has prognostic significance, Gut 69 (7) (2020) 1193–1205. https://doi:10.1136/gutjnl-2019-319639.
[35] C. Sebastian, C. Ferrer, M. Serra, et al., A non-dividing cell population with high pyruvate dehydrogenase kinase activity regulates metabolic heterogeneity and tumorigenesis in the intestine, Nat. Commun. 13 (1) (2022) 1503. https://doi:10.1038/s41467-022-29085-y.
[36] D.R. Schmidt, R. Patel, D.G. Kirsch, C.A. Lewis, M.G. Vander Heiden, J.W. Locasale, Metabolomics in cancer research and emerging applications in clinical oncology, CA A Cancer J. Clin. 71 (4) (2021) 333–358. https://doi:10.3322/caac.21670.
[37] M. Rossi, P. Altea-Manzano, M. Demicco, et al., PHGDH heterogeneity potentiates cancer cell dissemination and metastasis, Nature 605 (7911) (2022) 747–753. https://doi:10.1038/s41586-022-04758-2.
[38] P. Xie, H. Yan, Y. Gao, X. Li, D.-B. Zhou, Z.-Q. Liu, Construction of m6A-related lncRNA prognostic signature model and immunomodulatory effect in glioblastoma multiforme, Front. Oncol. 12 (2022), https://doi.org/10.3389/fonc.2022.920926.
[39] L. Cheng, X. Zhang, Y.-Z. Huang, et al., Metformin exhibits antiproliferation activity in breast cancer via miR-483-3p/METTL3/m6A/p21 pathway, Oncogenesis 10 (1) (2021) 7. https://doi:10.1038/s41389-020-00290-y.
[40] C.-J. Chen, J.-Y. Huang, J.-Q. Huang, et al., Metformin attenuates multiple myeloma cell proliferation and encourages apoptosis by suppressing METTL3-mediated m6A methylation of THRAP3, RBM25, and USP4, Cell Cycle 22 (8) (2023) 986–1004. https://doi:10.1080/15384101.2023.2170521.
[41] Y. Huang, R. Su, Y. Sheng, et al., Small-molecule targeting of oncogenic FTO demethylase in acute myeloid leukemia, Cancer Cell 35 (4) (2019) 677–691. https://doi:10.1016/j.ccell.2019.03.006.
[42] E. Yankova, W. Blackaby, M. Albertella, et al., Small-molecule inhibition of METTL3 as a strategy against myeloid leukaemia, Nature 593 (7860) (2021) 597–601. https://doi:10.1038/s41586-021-03536-w.